[AMERICAN JOURNAL OF SCIENCE, VOL. 257, APRIL 1959, P. 297-315]

PHASE EQUILIBRIA IN THE SYSTEM MANGANESE OXIDE—SiO_2 IN AIR*

ARNULF MUAN

Dept. of Metallurgy, Pennsylvania State University,
University Park, Pennsylvania

ABSTRACT. Phase relations in the system manganese oxide—SiO_2 in air have been investigated in the temperature range 990-1571°C, using the quenching technique. The data obtained permit the construction of a phase diagram showing stability relations in the liquidus temperature region as well as at subsolidus temperatures. For sake of simplicity the phase relations are illustrated in the form of a projection into a chosen join through the ternary system. The resulting diagram has the *appearance* of a binary system, with "binary invariant" situations as follows: a peritectic exists at 1230°C, with cubic Mn_3O_4, tephroite ($2MnO \cdot SiO_2$) and liquid coexisting in equilibrium with a gas phase of O_2 partial pressure equal to 0.21 atm. At 1206°C tephroite, $MnO \cdot SiO_2$ solid solution (rhodonite), liquid and gas are present together in what appears as an eutectic situation. Tridymite (SiO_2), $MnO \cdot SiO_2$(ss), liquid and gas exist together in equilibrium in an apparently peritectic situation at 1272°C, and cristobalite together with 2 liquids and gas are the equilibrium phases at approximately 1700°C. In the subsolidus region the following apparently invariant situations have been determined: at 1204°C cubic Mn_3O_4, tephroite and $MnO \cdot SiO_2$(ss) coexist in equilibrium with a gas phase of O_2 partial pressure equal to 0.21 atm. Tetragonal Mn_3O_4, a phase probably analogous to the mineral braunite (Mn_2O_3(ss)), and $MnO \cdot SiO_2$(ss) are in equilibrium with this gas at 1168°C, while at 1048°C Mn_2O_3(ss), $MnO \cdot SiO_2$(ss) and tridymite are the stable phases in air. In addition, "invariant" situations also result from the tridymite-cristobalite inversion at approximately 1470°C and the inversion from tetragonal to cubic Mn_3O_4 at approximately 1160°C.

INTRODUCTION

Phase equilibrium studies are generally recognized as being necessary first steps in any investigation aimed at improving our knowledge of heterogeneous reactions. Accurate measurements of chemical properties in such systems can be interpreted intelligently only if the system is well defined with respect to the phases present.

Oxide systems have been the center of interest of research workers in many different fields. Geochemists and petrologists have gathered a tremendous amount of phase equilibrium data which have enabled them to infer conditions governing the formation and existence of many minerals and rocks. Their studies have dealt mainly with combinations of oxides of noble gas type ions such as for instance SiO_2, Al_2O_3, CaO, MgO, Na_2O, K_2O, while data on most oxides of transition elements, such as for instance manganese oxides, are relatively scarce. This situation undoubtedly exists partly because the latter systems are more difficult to study experimentally, but also because transition elements in their natural occurrences frequently are present as sulfides rather than as oxides.

Oxides also play a very important role as one or more of the phases present in many high temperature industrial processes. Ceramists deal essentially with oxide materials, and their efforts have contributed significantly to our knowledge of oxide chemistry. It is natural that ceramists are interested primarily in the chemically very stable oxides of noble gas type ions, such as

* Contribution No. 58-10 from College of Mineral Industries, The Pennsylvania State University, University Park, Pennsylvania.

SiO_2, Al_2O_3, CaO, MgO, Na_2O, K_2O, in other words the same oxides as are studied by geochemists. In the field of metallurgy, however, one is mainly concerned with the extraction of metals from oxide raw materials, and hence oxides of *low* stability are the center of interest, such as for instance iron oxides and manganese oxides. The metallurgist cannot, however, overlook the importance of systems made up from among the more stable oxides, which form the constituents of the slag phase and also are used in the refractory linings of the furnaces.

The most important oxide by far among those of transition elements is iron oxide. Systems containing iron oxide as a component have been studied and restudied by metallurgists, geochemists and ceramists alike over the last 50 years. By comparison, very few studies have been made of systems where oxides of other transition elements are present. Among those of next importance both technologically as well as geologically is manganese oxide.

While data on the system Mn—O are gradually accumulating in another phase of our research efforts (Hahn and Muan, in press), the present work represents a first step in our investigation of the system Mn—Si—O. Because manganese occurs in different states of oxidation, the O_2 partial pressure of the gas phase must be controlled carefully in any investigation of a system where manganese oxides are present. We have chosen to start our study of manganese oxide—SiO_2 equilibria by investigating the system in air, that is at a constant O_2 partial pressure of 0.21 atm. In choosing this approach we are actually working along the irregularly curved 0.21 atm. O_2 isobaric section through the system Mn—Si—O. Equilibria along this section may be represented in a simplified manner by projecting the points representing compositions of condensed phases into a chosen join. We will present the results in terms of the components Mn_3O_4 and SiO_2. The resulting diagram has the appearance of a binary system. Apparently invariant situations in this system are actually intersections between the 0.21 atm. isobaric surface and univariant lines in the system Mn—Si—O. Along such liquidus univariant lines two crystalline phases, liquid and gas coexist in equilibrium, whereas a subsolidus univariant situation is characterized by the coexistence in equilibrium of three crystalline phases and a gas phase.

Previous Work

Although manganese silicates have attracted considerable attention among geochemists as well as metallurgists, no systematic study of phase relations in the system manganese oxide—SiO_2 in air has been reported in the literature.

The one end member in the system, SiO_2, of course has been the subject of numerous phase investigations over the past few decades, starting with the now classic work in 1913 by Fenner. In spite of all efforts since that time, doubt still exists as to certain of the important characteristics of this substance, particularly with respect to the stability relations of the tridymite phase. An impression of the present status of our knowledge of this system can be obtained by reading recent papers by Sosman (1955), Flörke (1956), Eitel (1957), Hill and Roy (1958).

The system Mn—O, unfortunately, has not been studied experimentally in

any great detail. Scattered equilibrium data and calorimetric data are available in the literature, from which Coughlin (1954) has tabulated the standard free energies of formation of the various manganese oxides as a function of temperature. Most of the values listed in these tables were obtained by addition and subtraction of large numbers, each of which is subject to considerable margins of error. Hence the stability relations of the manganese oxides depicted by Coughlin's tables are uncertain and should be considered only as rough approximations. Hahn and Muan (in press) have studied recently limited parts of the Mn—O system, particularly the equilibria between Mn_2O_3 and Mn_3O_4 and between Mn_3O_4 and MnO. Their data show that Mn_3O_4 is the stable crystalline phase of manganese oxide in air above 877°C and up to the melting temperature of 1567°C. At temperatures slightly below 877°C Mn_2O_3 is the stable phase in air. It is well known that Mn_3O_4 exists in two different stable modifications, one high temperature cubic form with spinel structure and one low temperature tetragonal form. The exact temperature at which these two modifications coexist in equilibrium is still not certain. A discussion of the problem appears in a recent publication by Van Hook and Keith (1958). They indicate that the most likely inversion temperature is approximately 1160°C. The oxide Mn_2O_3, likewise, has two established polymorphic forms, the α-Mn_2O_3 with "C"-type cubic structure (Zachariasen, 1928; Pauling and Shappell, 1930) and the γ-Mn_2O_3 with distorted spinel structure (Dubois, 1935). The latter modification, however, is unstable relative to the former and will not appear in our phase equilibrium diagram.

Some of the previous experimental phase equilibrium studies of mixtures of manganese oxide and silica have suffered from insufficient control of the O_2 partial pressure of the gas phase in equilibrium with the condensed phases. This is probably one of the reasons why such a confusing variety of phase diagrams for the system "manganese oxide—silica" have appeared in the literature (Doerinckel, 1911; Glaser, 1926; Herty, 1930; White, Howat and Hay, 1934). A diagram for the system manganese oxide—SiO_2 under controlled, strongly reducing, conditions was published in 1958 by Glasser, who used CO_2/H_2 mixtures in order to define more precisely the O_2 partial pressure of the gas phase.

A large number of descriptions of naturally occurring manganese minerals with a bearing on the present study are found in mineralogy textbooks (see for instance Dana's System of Mineralogy, 1944) and numerous publications. Papers of particular interest are those describing the mineralogy and geology of the Långban deposits in Sweden (Magnusson, 1924; Flink, 1926; Palache, 1929).

Experimental Method

General Procedure.—The phase relations were determined by the quenching method. Preheated mixtures of manganese oxide and silica were held in platinum containers in air at constant temperature until equilibrium was reached among crystalline, liquid and gas phases. The samples were then quenched rapidly to room temperature. Phases present were identified by x-ray and microscopic methods, and compositions of liquids at liquidus temperatures were determined by wet chemical analysis.

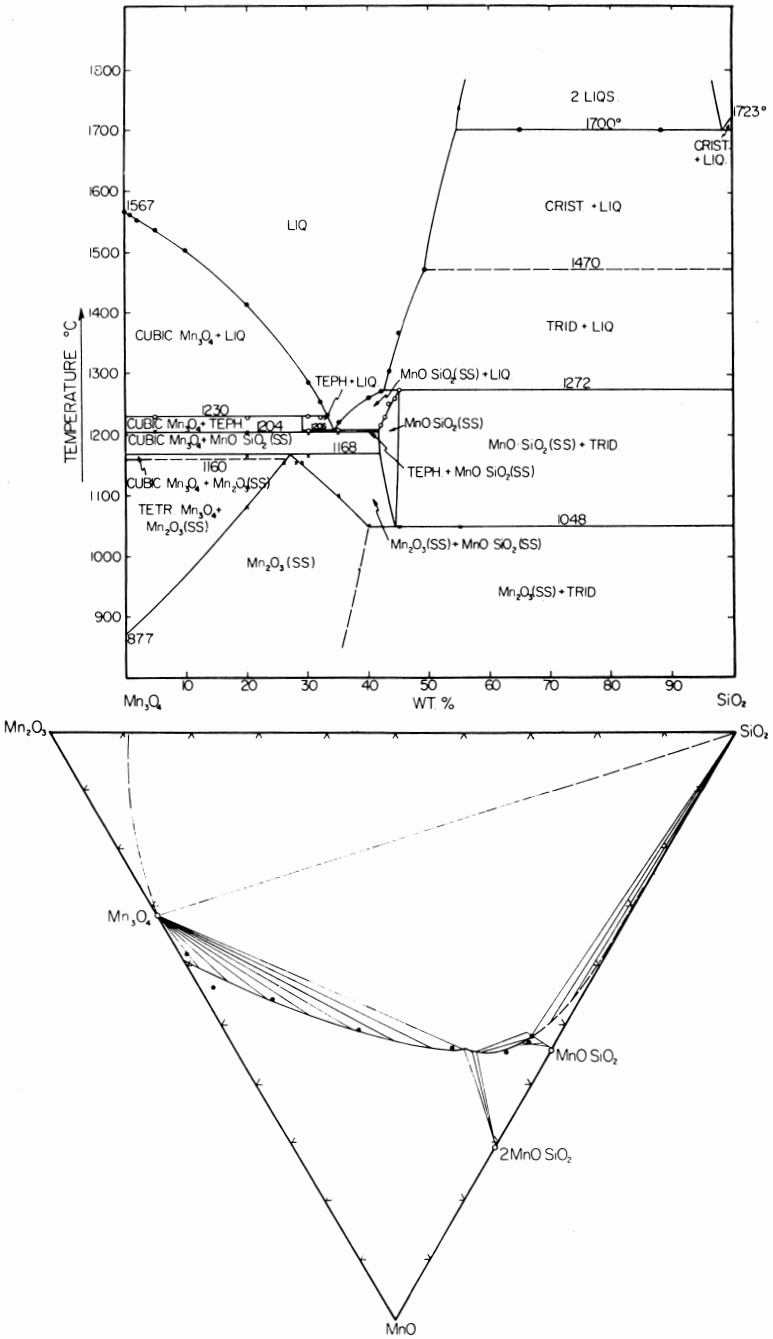

Fig. 1. Diagrams presented in order to show phase relations in the system manganese oxide—SiO_2 in air. The upper diagram has the appearance of a binary system, with

Materials.—Oxides of highest purity available commercially served as starting materials. The source of silica was c.p. silicic acid which was dehydrated by heating at 1300°C for 12 hours. The source of manganese oxide was "Baker Analyzed" grade manganese dioxide, MnO_2. Samples weighing 10 g were made up by mixing these materials in required proportions and mechanically grinding the mixture. Each mixture was then heated slowly to melting either in air atmosphere in a globar furnace, or in a gas-air combustion furnace in case of higher melting mixtures. The heating of the starting materials had to be carried out with utmost caution in slow steps from low temperature up to the liquidus region because the successive decomposition of higher to lower manganese oxides took place very violently. Particularly troublesome in this respect was the temperature region in which the first liquids form. These preheated and quenched mixtures, after grinding to minus 60 mesh, were used for the equilibration runs for determination of liquidus temperatures.

The same mixtures were usually used for determination of boundary curves also in the subsolidus temperature region. As a check on attainment of true equilibrium a few runs in this region were made with two different starting materials prepared by prolonged heating of the mixtures, one at temperatures slightly above and one at a temperature slightly below that of the boundary curve.

Furnaces and Temperature Control.—Vertical tube furnaces with windings of platinum or 80 platinum-20 wt. % rhodium were used for most of the quenching experiments. A modified Roberts and Morey (1930) strip furnace, using strip resistors of a 60 platinum-40 wt. % rhodium alloy, was used for a few quench runs at temperatures above 1600°C.

Temperatures in the vertical tube furnaces were measured before and after each run with a platinum 90–platinum-10 wt. % rhodium thermocouple frequently calibrated at melting points defined as follows: Au, 1063°C; $CaMgSi_2O_6$. 1391.5°C; $CaSiO_3$, 1544°C. Literature values for temperatures on the Geophysical Laboratory scale are used without correction up to 1550°C, the upper limit of the original scale. Temperatures above 1550°C are adjusted to the 1948 International Scale using the correction data tabulated by Corruccini (1949) and by Sosman (1952). Furnace temperature was controlled by a second thermocouple inserted close to the heating element and connected through compensating lead wires to a Celectray controller. The temperature

---

Mn_3O_4 and SiO_2 chosen as components. This part of the figure shows phases present as a function of temperature and manganese oxide to silica ratios of the mixtures. Heavy lines are boundary curves. These are dashed in regions where experimental data are less reliable or lacking. Solid dots, solid triangle, open circles and crosses represent experimentally determined points on liquidus, 2 liquid, solidus and subsolidus boundary curves, respectively, based on data contained in table 1. The lower, triangular diagram shows true compositions of liquid and crystalline phases expressed in terms of the chosen components MnO, Mn_2O_3 and SiO_2. Solid dots represent experimentally determined compositions of liquids at liquidus temperatures, and the heavy curve is the 0.21 atm. liquidus isobar drawn through these points. Light straight lines indicate approximate locations of conjugation lines connecting points representing compositions of liquids with points representing composition of crystalline phases with which the liquids are in equilibrium. Light dash curves are used to indicate how the Mn_3O_4—SiO_2 join is swung up to the Mn_2O_3—SiO_2 join for projection purposes, as explained in the text.

gradient at the hot spot did not exceed 2°C over 1 inch at 1300°C. Temperatures on the strip furnace were measured with an optical pyrometer calibrated at melting points defined as follows: $CaSiO_3$, 1544°C; 10 CaO 90 wt. % SiO_2, 1708°C; Pt, 1769°C.

Examination of Quenched Samples.—Phase identification in the liquidus temperature region was most easily accomplished with the microscope, using transmitted as well as reflected light techniques. The examination of polished sections in reflected light was particularly useful for distinguishing primary crystals from quench crystals in the manganese oxide rich part of the system. The identity of the phases was further confirmed by x-ray techniques, using Fe radiation with a Norelco spectrometer unit. The x-ray technique was also used for determination of compositions of solid solution crystalline phases in the subsolidus temperature region.

In order to determine the compositions of liquids at liquidus temperatures it was necessary to carry out chemical analysis of quenched samples. After crushing of these samples, suitable amounts (~0.2 g) were weighed and transferred to a platinum container. Excess standard ferrous ammonium sulfate solution was added together with 5 ml concentrated H_2SO_4, and the solution was boiled for a couple of minutes. After cooling, 10 ml of HF was added, a cover was put on the crucible and the solution boiled until the sample was completely dissolved, which usually required a period of approximately 10 minutes. The crucible was plunged into a 600 ml beaker containing 250 ml water and 10 ml 1:1 H_2SO_4. After saturation with boric acid, the solution was titrated with 0.05 – n $KMnO_4$.

RESULTS

Results of quenching experiments are listed in table 1 and illustrated graphically in figure 1. This figure consists of 2 diagrams. The upper diagram with the appearance of a binary system shows phases present as a function of temperature. Because the compositions of all condensed phases cannot be represented in terms of the two chosen components, a supplementary diagram is presented in the lower half of the figure. This ternary diagram shows true compositions of condensed phases in equilibrium along boundary curves in the upper diagram.

The most important features of the diagrams are as follows: liquidus temperatures are high at both ends of the system, 1567 and 1723°C being the melting temperatures in air of manganese oxide and cristobalite, respectively. In the silica rich end of the system, liquidus temperatures remain high (~1700°C) until a composition of 50 Wt.% manganese oxide is reached, corresponding to the maximum extent of liquid immiscibility. As the manganese oxide content increases above this value, liquidus temperatures fall off sharply. The $MnO \cdot SiO_2$(ss)-tridymite boundary curve is crossed by the 0.21 atm. O_2 isobar at 1272°C in what appears as a peritectic situation in the upper diagram of figure 1. The lowest liquidus temperature in air is 1206°C, with $MnO \cdot SiO_2$(ss) and tephroite coexisting with a liquid containing 66 Wt.% manganese oxide and 34 Wt.% SiO_2. As the manganese oxide content increases above this level, liquidus temperatures start rising, and another "peritectic"

situation prevails at 1230°C. with tephroite and Mn_3O_4 as the crystalline phases present in equilibrium with liquid. In the composition range between 67 and 100 Wt.% Mn_3O_4, cubic Mn_3O_4 is the primary crystalline phase.

Tephroite is stable in air in the temperature interval 1204-1230°C. At the upper temperature limit of stability it decomposes incongruently to Mn_3O_4 and liquid; at the lower temperature limit of stability it decomposes to Mn_3O_4 and $MnO \cdot SiO_2$(ss). The phases Mn_3O_4 and $MnO \cdot SiO_2$(ss) coexist in equilibrium down to 1168°C in air. At this temperature Mn_2O_3(ss) becomes stable and the condensed phases present are either $Mn_3O_4 + Mn_2O_3$(ss) or Mn_2O_3(ss) $+ MnO \cdot SiO_2$(ss) at temperatures below 1168°C, depending on the SiO_2 content of the mixture. The $MnO \cdot SiO_2$(ss) phase exists in stable equilibrium in air down to 1048°C. Below this temperature it decomposes to Mn_2O_3(ss) and tridymite. Tetragonal Mn_3O_4 exists as an equilibrium phase in air down to a minimum temperature of 877°C. Below this temperature pure Mn_3O_4 is oxidized to Mn_2O_3; this transformation temperature increases to a maximum of 1168°C as the SiO_2 content of the mixture increases.

A summary of "invariant" situations in the system manganese oxide—SiO_2 in air is presented in table 2, and powder x-ray diffraction data for manganese oxide containing crystalline phases are listed in table 3.

DISCUSSION

The most interesting feature of the phase relations in this system is the stable existence of a SiO_2-containing solid solution phase with α–Mn_2O_3 structure. The large increase in the transformation temperature of Mn_2O_3 to Mn_3O_4 as SiO_2 is added to manganese oxide shows conclusively that SiO_2 enters the structure of the latter. The phase formed is termed Mn_2O_3(ss) in this paper, leaving the question open as to the exact nature of the solid solution. The x-ray patterns show no appreciable shift in the d-spacings of the main lines of Mn_2O_3 as SiO_2 content increases, but some weak extra lines appear, indicating some degree of ordered substitution rather than a completely random distribution of the cations.

The Mn_2O_3(ss) phase appears to be identical to the naturally occurring mineral braunite, which has been described and studied by a large number of investigators in the past. Structure determinations by x-ray diffraction studies have been reported by Aminoff (1931) and by Byström and Mason (1943). The structures as well as d-spacings are very similar to those for the pure Mn_2O_3 end member, which has a C-type sesquioxide structure according to studies carried out by Zachariasen (1928) and by Pauling and Shappell (1930).

The way in which Si^{4+} ions are accommodated in the Mn_2O_3 structure in the mineral braunite has been the subject of a great deal of speculation and some investigations. In natural occurrences the composition of this mineral seems to be close to the formula $3Mn_2O_3 \cdot MnSiO_3$, corresponding to approximately 10 Wt.% SiO_2, although slight variations in this ratio as well as presence of other oxides in the structure are often encountered. Analytical data for this mineral are summarized in Dana's System of Mineralogy (1944). The authors of this book are careful to point out that the exact mechanism of the

substitution is unknown. Goldschmidt (1954), however, states categorically that "braunite is not contaminated manganese sesquioxide but the compound $3Mn_2O_3 \cdot MnSiO_3$".

Some recent magnetic and chemical studies have shed new light on this problem. Fyfe (1949) has developed a chemical test for the presence of trivalent manganese, based on the formation of a stable complex ion with acetylacetone. He found that a–Mn_2O_3 gives the reaction of $Mn^{2+} + Mn^{4+}$, whereas γ–Mn_2O_3, studied for comparison, reacts as 2 Mn^{3+}. Krishnan and Banerjee (1939) have made magnetic measurements on natural braunites to determine the oxidation state of manganese in this phase. Magnetic susceptibility measurements were non-conclusive, because the magnetic moment of Mn^{3+}, 4.90 Bohr magnetons, is almost midway between the moments of Mn^{2+} and Mn^{4+}, 5.92 and 3.87 Bohr magnetons, respectively. However, measurements of the magnetic anisotropy of the braunite revealed that the manganese was present as $Mn^{2+} + Mn^{4+}$ rather than as Mn^{3+}. Krishnan and Banerjee therefore suggest that the formula for braunite be written $3MnMnO_3 \cdot MnSiO_3$ as against the usual formula $3Mn_2O_3 \cdot MnSiO_3$.

The present investigation definitely establishes that a wide range of compositions is possible in braunite, from pure Mn_2O_3 as one end member to a silica content of at least 40 Wt.% SiO_2. It appears likely that the mechanism

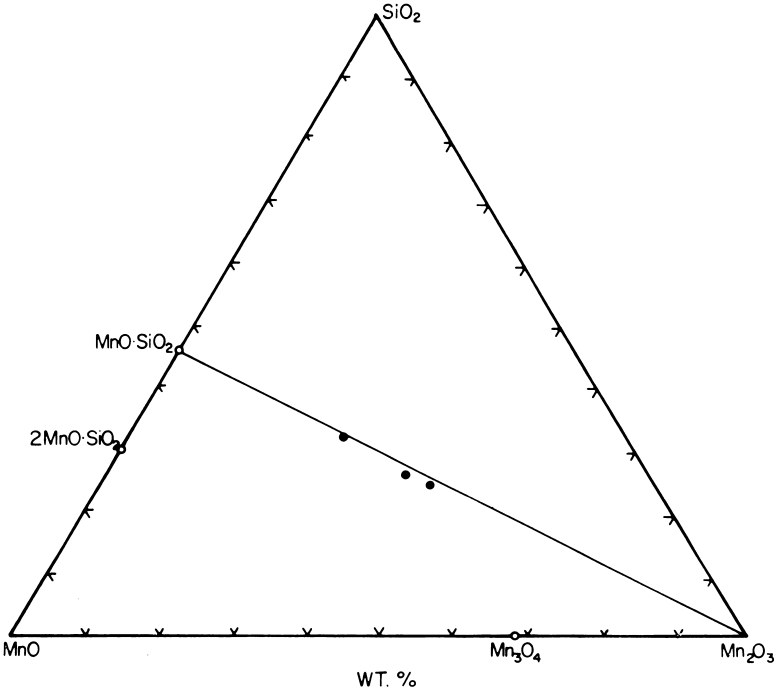

Fig. 2. Diagram showing compositions of Mn_2O_3(ss) crystals in air at 1000°C (solid dots). The light straight lines is the join $MnO \cdot SiO_2$—Mn_2O_3 (compare discussion in text).

for the solid solution formation is a substitution of Si^{4+} for Mn^{4+} in the Mn_2O_3 lattice. The present data give strong support for the assumption that Mn_2O_3 consists of divalent and tetravalent manganese rather than trivalent manganese, for the continuous and extensive solid solution established for Mn_2O_3(ss) is most likely explained by assuming the formula $Mn^{2+}\ Mn^{4+}\ O_3$.

A further support of the assumption that the Mn_2O_3(ss) crystals can be considered a solid solution $Mn^{2+}(Mn^{4+}Si^{4+})O_3$ is offered by the results of chemical analysis shown in figure 2. Compositions of Mn_2O_3(ss) crystals (solid dots) prepared by heating manganese oxide—SiO_2 mixtures in air for 200 hours at 1000°C fall close to the join $MnO \cdot SiO_2$—Mn_2O_3 as predicted by the mechanism of substitution suggested above.

The crystalline phases tephroite ($2MnO \cdot SiO_2$), tridymite (SiO_2), cristobalite (SiO_2) and Mn_3O_4 appear to be pure phases corresponding to the chemical formulas written above, as closely as could be determined with the experimental techniques used (x-ray and microscopic examination as well as phase evidence). The phase designated $MnO \cdot SiO_2$(ss), after quenching to room temperature, is closely similar to the naturally occurring mineral rhodonite. A small excess of manganese over the stoichiometric 1:1 ratio is permitted in this structure, giving rise to a solid solution one-phase area (labeled $MnO \cdot SiO_2$(ss)) in the upper diagram in figure 1. No high temperature x-ray examination of this phase was carried out in the present investigation. In view of the complexity of the structure of metasilicates (compare for instance extensive studies of the magnesium analogue, $MgO \cdot SiO_2$ (Atlas, 1952)), an x-ray study of the $MnO \cdot SiO_2$(ss) phase as a function of O_2 partial pressure and thermal history is a research problem in itself. In the present paper the phase is referred to as $MnO \cdot SiO_2$(ss), leaving open the question as to the exact crystal structure of this phase.

Another notable feature of the phase relations in this system is the stable existence in air of tephroite as well as $MnO \cdot SiO_2$(ss) at liquidus temperatures, both phases containing essentially all manganese as Mn^{2+}. This situation is completely different from the one prevailing in the system iron oxide—SiO_2, where magnetite (Fe_3O_4) and silica (cristobalite or tridymite) are the only crystalline phases present in equilibrium at liquidus temperatures in air. In other words, Mn^{2+} is much more stable relative to the other valence states of manganese than Fe^{2+} is relative to Fe^{3+}. The extreme stability of Mn^{2+} in oxide phases is of course inherent in the numerical values listed in the free energy tables compiled by Coughlin (1954).

As temperature is lowered, a tendency for oxidation of Mn^{2+} to higher valence states prevails, because this is a strongly exothermic reaction. Tephroite oxidizes at temperatures only slightly below the lowest liquidus temperature in the system, first to Mn_3O_4 plus $MnO \cdot SiO_2$(ss), and subsequently to Mn_2O_3(ss). The $MnO \cdot SiO_2$(ss) phase persists in air down to a temperature of 1048°C before oxidation to Mn_2O_3(ss) and tridymite takes place.

The boundary curve between the fields of tridymite and cristobalite has been dashed at 1470°C in accordance with the "classical" picture of stability relations among the various modifications (Fenner, 1913), and assuming no solid solution in tridymite or cristobalite. No consistent data regarding the

relative stabilities of these phases in the present system were obtained in runs of 2 days duration. Tridymite always formed at temperatures below 1480°C and cristobalite above this temperature in a mixture containing 40 Wt.% manganese oxide, while cristobalite was the phase always forming in the temperature interval 1430-1475°C in a mixture containing 8 Wt.% manganese oxide.

The incongruent melting of tephroite in air as distinguished from the congruent melting found by Glasser (1958) for this phase under strongly reducing conditions is a noteworthy feature. It is probable that the discrepancies in previous literature regarding the melting relations of this phase are due to unsatisfactory methods for controlling and maintaining the desired level of O_2 pressures in the gas phase. These relations are likely to be better understood upon completion of studies of the system $MnO—Mn_2O_3—SiO_2$ at various O_2 partial pressures now in progress in our laboratories.

The extremely strong stabilizing effect of SiO_2 on Mn^{2+} relative to the higher valence states of manganese in melts becomes apparent by an inspection of the composition curve for the liquid in the lower half of figure 1. This curve is for liquids at liquidus temperatures in air, hence temperature is a variable in addition to composition (silica to manganese oxide ratio). The effect of temperature is simple: Because the oxidation of Mn^{2+} is exothermic, a decrease in temperature causes a decrease in the Mn^{2+}/Mn^{3+} ratio. Referring to figure 1 it will be noticed that a pure manganese oxide liquid in air at temperature slightly above the liquidus consists of approximately 40 Wt.% MnO and 60 Wt.% Mn_2O_3. As SiO_2 is added, liquidus temperatures decrease (see upper half of fig. 1). If temperature were the only factor determining the Mn^{2+}/Mn^{3+} equilibrium, this ratio would be expected to decrease as silica is added, corresponding to a curve originating at the 40 MnO 60 Wt.% Mn_2O_3 composition point and located on the Mn_2O_3 side of the straight line connecting this point with the SiO_2 corner of the triangle in figure 1. The actual curve, however, bends sharply to the opposite side of this straight line. This situation is a result of the strong effect of acidity[1] on the Mn^{2+}/Mn^{3+} equilibrium. As the acidity of the system increases with increasing SiO_2 content, the Mn^{2+} is stabilized relative to Mn^{3+}, and so strong is this stabilizing effect of SiO_2 that it completely overshadows the opposite effect on the Mn^{2+}/Mn^{3+} equilibrium of decreasing temperatures. Hence the 0.21 atm. O_2 isobar along the liquidus surface has the course represented by the heavy curve in the lower half of figure 1. The slope of this curve varies continuously, except where a boundary curve is crossed.

The composition of the silica-rich liquid in the region of equilibrium coexistence of two immiscible liquids was only estimated roughly. The refractive index of the glass was not significantly larger than that of pure SiO_2 glass, and the manganese oxide content is judged not to exceed 1 Wt.%.

The relation between a diagram drawn with the appearance of a binary system, such as the join $Mn_3O_4—SiO_2$ represented in the upper half of figure 1, and the ternary system $MnO—Mn_2O_3—SiO_2$ represented in the lower, tri-

[1] For a discussion of acid-base relations in silicate liquids, see for instance a recent paper by Weyl (1956).

angular diagram in figure 1. has been explained in detail in previous papers by this author dealing with phase equilibria in iron oxide containing silicate systems (Muan, 1955, 1957, 1958). The same methods described in those papers have been used for projecting composition points from the lower ternary system up to the "binary" join in figure 1. Straight lines are drawn through composition points with a direction toward the O corner of the triangle representing the system Mn—Si—O. These lines are "reaction lines" describing changes in total composition of condensed phases as these react with O_2 of the gas phase in response to temperature changes. The intersections between these reaction lines and the Mn_3O_4—SiO_2 join in the lower triangular diagram are taken to represent compositions of condensed phases in the upper simplified "binary" diagram. These points are projected to the upper, binary join by first swinging the Mn_3O_4—SiO_2 join in the triangle around the SiO_2 corner upward until it falls on the Mn_2O_3—SiO_2 join, and then displacing the points along vertical lines to the upper half of the figure.

When using and interpreting the "binary" phase diagram in the upper part of figure 1 it is important to keep in mind its relation to the ternary system. Although it is true that compositions of condensed phases cannot be expressed in terms of two chosen components, such as Mn_3O_4 and SiO_2, nevertheless this diagram can be treated like a binary system as far as path of crystallization is concerned. The oxygen of the atmosphere (air) reacts with the condensed phases to keep the liquid compositions along the 0.21 atm. O_2 isobaric curve regardless of the nature of the crystalline phases separating out. Hence an apparently invariant situation will exist where the 0.21 atm. O_2 isobar crosses a boundary curve. Only at one temperature, at the given O_2 partial pressure, can two crystalline phases and a liquid coexist in equilibrium, because one degree of freedom has been "used up" in choosing air as the atmosphere. Consequently, intersections between the 0.21 atm. O_2 isobar and univariant lines in the system Mn—Si—O appear as invariant situations in the upper "binary" system.

An extensive discussion of the application of phase equilibria in the system manganese oxide-silica to geochemical and technological problems must await results of studies presently in progress in our laboratories at various O_2 partial pressures. However, a few general remarks may be made. The relatively constant ratio of silica to manganese oxide in naturally occurring braunites is an interesting observation which may perhaps be used to infer some of the conditions existing during the formation of this phase in nature. The composition limits of braunite depend primarily on two parameters, temperature and O_2 partial pressure. As O_2 partial pressure is reduced, the Mn_2O_3 to Mn_3O_4 decomposition temperature decreases, and the two boundary curves in figure 1, representing compositions of braunite in equilibrium with Mn_3O_4 and $MnO \cdot SiO_2$(ss), respectively, move downward. Hence the "peak" at which these lines meet also moves downward with decreasing O_2 pressure, and the composition of the braunite phase in terms of silica to manganese oxide ratio at this peak may also vary. These relations are illustrated in the sketch in figure 3. If a naturally occurring braunite has been formed at a temperature close to the "peak" under the prevailing conditions of

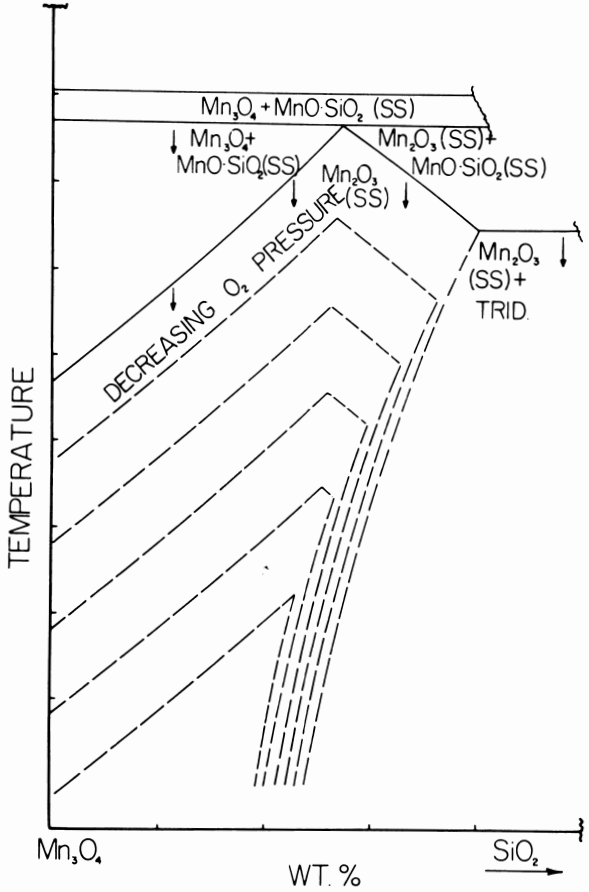

Fig. 3. Sketch presented in order to indicate probable changes in composition range of Mn_2O_3(ss) as O_2 partial pressure is decreased below that of air (compare discussion in text).

O_2 partial pressure, its composition range should be very narrow. Moreover, if the shift in the "peak" composition is known as a function of temperature and O_2 partial pressure from laboratory examinations, a close estimate of the values of these parameters at the time of formation of the mineral assemblage may be possible. Although slow reaction rates probably will prevent an experimental study of these reactions down to temperatures much below 1000°C, an attempt to map out the composition limits of the braunite phase volume seems like a worthwhile subject for future research.

SUMMARY

A start has been made on the investigation of phase equilibria in the system Mn—Si—O by working along the 0.21 atm. O_2 isobaric section through this system at a total pressure of 1 atm. The phase relations are

represented in an *apparently* binary diagram (Mn_3O_4—SiO_2) showing phases present as a function of temperature, and a supplementary diagram showing true compositions of condensed phases. Intersections between the 0.21 atm. O_2 isobar and boundary curves on the liquidus surface correspond to liquidus univariant situations in the ternary system characterized by the equilibrium coexistence of two crystalline, one liquid and a gas phase, or one crystalline, two liquid and a gas phase. However, because the O_2 partial pressure of the latter has been chosen, the existing degree of freedom has been "used up", and the presence of these phases in equilibrium appears as invariant situations in the system drawn as the "binary" system Mn_3O_4—SiO_3 for sake of simplification. Similarly, subsolidus ternary univariant situations in the system Mn—Si—O, with 3 crystalline phases and gas existing together in equilibrium, appear as invariant situations in the simplified "binary" diagram.

The "binary" system and the "invariant" situations are characterized as follows: manganese oxide melts at 1567°C in air, cubic Mn_3O_4 being the primary crystalline phase. Liquidus temperatures decrease sharply as SiO_2 is added A "peritectic" situation exists at 1230°C with Mn_3O_4, tephroite and a liquid of composition 54MnO, $13Mn_2O_3$, 33 Wt.% SiO_2 present together in equilibrium with the gas. At 1206°C tephroite, $MnO \cdot SiO_2$(ss) (rhodonite), a liquid of composition 54MnO, $12Mn_2O_3$, 34 Wt.% SiO_2 and gas coexist in equilibrium in what appears to be an eutectic situation. With SiO_2 contents increasing above 34 Wt.%, liquidus temperatures start rising, $MnO \cdot SiO_2$(ss) being the primary crystalline phase in the composition range 34-42 Wt.% SiO_2. At 1272°C another apparently peritectic sitaution prevails, with $MnO \cdot SiO_2$(ss), tridymite and liquid of composition 53MnO, $5Mn_2O_3$, 42 Wt.% SiO_2 existing together in equilibrium in air. As SiO_2 content increases still farther, liquidus temperatures rise very steeply toward a plateau at 1700°C caused by the presence of two immiscible liquids over the composition range 55-99 Wt.% SiO_2 at liquidus temperatures. The melting point of pure SiO_2 (cristobalite) is 1723°C. Phase transformation in Mn_3O_4 and oxidation-reduction equilibria give rise to four apparently invariant situations in the subsolidus region of the system in the temperature range investigated. At 1204°C Mn_3O_4, tephroite and $MnO \cdot SiO_2$(ss) coexist in equilibrium in air. At 1168°C the following crystalline phases exist together in equilibrium: cubic Mn_3O_4, Mn_2O_3(ss) and $MnO \cdot SiO_2$(ss). At 1160°C another "invariant" situation exists as the tetragonal and cubic forms of Mn_3O_4 are present together with Mn_2O_3(ss) and gas. The phase $MnO \cdot SiO_2$(ss) is stable in air down to 1048°C. At this temperature it decomposes to Mn_2O_3(ss) and tridymite in an apparently eutectoid situation.

The presence of tephroite and $MnO \cdot SiO_2$(ss) as the equilibrium phases at liquidus temperatures in air shows the extreme stability of the Mn^{2+} ion and accounts for its occurrence almost to the exclusion of manganese ions of higher valence states in igneous minerals and rocks. The Mn_2O_3(ss) crystals appearing as one of the equilibrium phases in the subsolidus temperature region seem to be the synthetic analogues of the naturally occurring mineral braunite, "$3Mn_2O_3 \cdot MnSiO_3$". A large range of manganese oxide to silica ratios in this phase has been found in the present investigation, strongly sug-

gesting a subsitution of Si^{4+} for Mn^{4+} in the lattice of α–Mn_2O_3. In accordance with this observation and previous evidence from chemical as well as magnetic tests the α-form of Mn_2O_3 is probably best represented by the formula $(Mn^{2+}\ Mn^{4+})O_3$. and the braunite formula should be written more appropriately $Mn^{2+}\ (Mn^{4+}.\ Si^{4+})O_3$. Compositions of natural braunites should depend mainly on temperature and O_2 partial pressure existing during formation of the mineral. Further laboratory work on composition limits for the Mn_2O_3(ss) phase as a function of temperature and O_2 partial pressure, combined with chemical and petrographic analyses of braunite in manganese deposits, may shed some new light on the conditions of formation of these deposits.

ACKNOWLEDGMENTS

The assistance of T. Ranganathan and A. M. Byström in carrying out and supervising the chemical analysis, respectively, is gratefully acknowledged. This work was carried out as part of a research project sponsored by the American Iron and Steel Institute following the recommendation of the Research Subcommittee of the Refractories Committee. The author wishes to acknowledge the many helpful suggestions made by E. F. Osborn during the preparation of this manuscript.

TABLE 1

Results of Quenching Experiments

Temp. of Quenching Run (°C)	Phases Present*	Temp. of Run for Anal. (°C)	Initial Comp. (Wt.%) Mn_3O_4	Initial Comp. (Wt.%) SiO_2	Comp. After Equilibration (Wt.%) MnO	Comp. After Equilibration (Wt.%) Mn_2O_3	Comp. After Equilibration (Wt.%) SiO_2
1571	Liq.	1577	100	0			
1565	Mn_3O_4						
1565	Liq.	1574	99	1	38	61	1
1559	Mn_3O_4 + Liq.						
1256	Mn_3O_4 + Liq.						
1213	Mn_3O_4 + Teph.						
1194	Mn_3O_4 + $MnO \cdot SiO_2$(ss)						
1096	Mn_3O_4 + Mn_2O_3(ss)						
1557	Liq.	1566	98	2	44	54	2
1547	Mn_3O_4 + Liq.						
1539	Liq.	1551	95	5	51	44	5
1534	Mn_3O_4 + Liq.						
1234	Mn_3O_4 + Liq.						
1225	Mn_3O_4 + Teph.						
1208	Mn_3O_4 + Teph.						
1201	Mn_3O_4 + $MnO \cdot SiO_2$(ss)						
1508	Liq.	1515	90	10	45	45	10
1500	Mn_3O_4 (tr.) + Liq.						
1488	Mn_3O_4 + Liq.						
1160	Mn_3O_4 + Mn_2O_3 (ss)						
1000	Mn_3O_4 + Mn_2O_3 (ss)						

TABLE 1 (Continued)

Temp. of Quenching Run (°C)	Phases Present*	Temp. of Run for Anal. (°C)	Initial Comp. (Wt.%) Mn_3O_4	SiO_2	Comp. After Equilibration (Wt.%) MnO	Mn_2O_3	SiO_2
1417	Liq.	1420	80	20	51	29	20
1412	Mn_3O_4 + Liq.						
1233	Mn_3O_4 + Liq.						
1223	Mn_3O_4 + Teph.						
1204	Mn_3O_4 + Teph. + $MnO \cdot SiO_2$(ss)						
1194	Mn_3O_4 + $MnO \cdot SiO_2$(ss)						
1170	Mn_3O_4 + $MnO \cdot SiO_2$(ss)						
1161	Mn_3O_4 + Mn_2O_3(ss)						
1094	Mn_3O_4 (tr.) + Mn_2O_3(ss)						
1070	Mn_2O_3(ss)						
1000	Mn_2O_3(ss)						
1070	Mn_2O_3(ss)		78	22			
1164	Mn_3O_4 + Mn_2O_3(ss)		76	24			
1144	Mn_3O_4 + Mn_2O_3(ss)						
1094	Mn_2O_3(ss)						
1164	Mn_3O_4 (tr.) + Mn_2O_3(ss)		74	26			
1144	Mn_2O_3(ss)						
1226	Mn_3O_4 + Teph.		72	28			
1164	Mn_2O_3(ss) + $MnO \cdot SiO_2$(ss) (tr.)						
1144	Mn_2O_3(ss)						
1170	Mn_3O_4 + $MnO \cdot SiO_2$(ss)	1315	71	29	58	13	29
1164	Mn_2O_3(ss) + $MnO \cdot SiO_2$(ss)						
1144	Mn_2O_3(ss)						
1292	Liq.	1297	70	30	59	11	30
1277	Mn_3O_4 + Liq.						
1232	Mn_3O_4 + Liq.						
1227	Teph. + Liq.						
1208	Teph. + Liq.						
1206	Teph. + $MnO \cdot SiO_2$(ss) + Liq.						
1204	Mn_3O_4 + Teph. + $MnO \cdot SiO_2$(ss)						
1194	Mn_3O_4 + $MnO \cdot SiO_2$(ss)						
1170	Mn_3O_4 + $MnO \cdot SiO_2$(ss)						
1160	Mn_2O_3(ss) + $MnO \cdot SiO_2$(ss)						
1094	Mn_2O_3(ss)						
1257	Liq.	1260	68	32	53	15	32
1249	Mn_3O_4 + Liq.						
1233	Mn_3O_4 + Liq.						
1223	Teph. + Liq.						
1164	Mn_2O_3(ss) + $MnO \cdot SiO_2$(ss)						
1220	$MnO \cdot SiO_2$(ss) (tr.) + Liq.		65	35			
1207	$MnO \cdot SiO_2$(ss) + Liq.						
1205	Teph. + $MnO \cdot SiO_2$(ss)						
1203	Mn_3O_4 + Teph. + $MnO \cdot SiO_2$(ss)						
1200	Mn_3O_4 + $MnO \cdot SiO_2$(ss)						
1160	Mn_2O_3(ss) + $MnO \cdot SiO_2$(ss)						
1107	Mn_2O_3(ss) + $MnO \cdot SiO_2$(ss)						
1094	Mn_2O_3(ss)						

TABLE 1 (Continued)

Temp. of Quenching Run (°C)	Phases Present*	Temp. of Run for Anal. (°C)	Initial Comp. (Wt.%) Mn_3O_4	SiO_2	Comp. After Equilibration (Wt.%) MnO	Mn_2O_3	SiO_2
1264	Liq.	1269	60	40	53.5	6.5	40
1255	$MnO \cdot SiO_2$(ss) + Liq.						
1160	Mn_2O_3(ss) + $MnO \cdot SiO_2$(ss)						
1060	Mn_2O_3(ss) + $MnO \cdot SiO_2$(ss)						
1040	Mn_2O_3(ss) + Trid.						
1025	Mn_2O_3(ss) + Trid.						
1280	Liq.		58	42			
1270	$MnO \cdot SiO_2$(ss) (tr.) + Liq.						
1264	$MnO \cdot SiO_2$(ss) + Liq.						
1220	$MnO \cdot SiO_2$(ss) + Liq.						
1211	$MnO \cdot SiO_2$(ss)						
1240	$MnO \cdot SiO_2$(ss) + Liq.		57.4	42.6			
1217	$MnO \cdot SiO_2$(ss)						
1180	$MnO \cdot SiO_2$(ss)						
1094	Mn_2O_3(ss) + $MnO \cdot SiO_2$(ss)						
1308	Liq.	1311	56.7	43.3	52	4	44
1298	Trid. (tr.) + Liq.						
1277	Trid. + Liq.						
1271	$MnO \cdot SiO_2$(ss) + Liq.						
1250	$MnO \cdot SiO_2$(ss) + Liq. (tr.)						
1220	$MnO \cdot SiO_2$(ss)						
1180	$MnO \cdot SiO_2$(ss)						
1094	$MnO \cdot SiO_2$(ss)						
1259	$MnO \cdot SiO_2$(ss) + Liq. (tr.)		55.7	44.3			
1220	$MnO \cdot SiO_2$(ss)						
1180	$MnO \cdot SiO_2$(ss)						
1094	$MnO \cdot SiO_2$(ss)						
1404	Liq.	1381	55	45	51	4	45
1366	Trid. (tr.) + Liq.						
1342	Trid. + Liq.						
1277	Trid. + Liq.						
1269	$MnO \cdot SiO_2$(ss)						
1160	$MnO \cdot SiO_2$(ss) + Trid. (tr.)						
1080	$MnO \cdot SiO_2$(ss) + Trid. (tr.)						
1051	$MnO \cdot SiO_2$(ss) + Trid. (tr.)						
1045	Mn_2O_3(ss) + Trid.						
990	Mn_2O_3(ss) + Trid.						
1760	Liq.		50.8	49.2			
1488	Liq.						
1471	Trid. (tr.) + Liq.						
1760	Liq.		45	55			
1710	$Liq._1$ + $Liq._2$ (tr.)						
1660	Crist. + Liq.						
1518	Crist. + Liq.						
1400	Trid. + Liq.						
1056	Trid. + $MnO \cdot SiO_2$(ss)						
1042	Trid. + Mn_2O_3(ss)						
1496	Trid. + Crist. + Liq.		40.6	59.4			
1461	Trid. + Liq.						

TABLE 1 (Continued)

Temp. of Quenching Run (°C)	Phases Present*	Temp. of Run for Anal. (°C)	Initial Comp. (Wt.%) Mn_3O_4	SiO_2	Comp. After Equilibration (Wt.%) MnO	Mn_2O_3	SiO_2
1760	Liq.$_1$ + Liq.$_2$		35	65			
1708	Liq.$_1$ + Liq.$_2$						
1692	Crist. + Liq.						
1620	Crist. + Liq.						
1496	Trid. + Liq.						
1710	Liq.$_1$ + Liq.$_2$		12	88			
1690	Crist. + Liq.						
1475	Crist. + Liq.						
1430	Crist. + Liq.						

* Abbreviations used in this and succeeding tables have the following meanings: Teph. = crystals of tephroite ($2MnO \cdot SiO_2$); Crist. = crystals of cristobalite; Trid. = crystals of tridymite; Liq. = liquid; tr. = trace; (ss) = solid solution.

Summary of "Invariant"* Situations in the System Manganese Oxide—SiO_2 in Air

Phases Present	Comp. of Liquid (Wt.%) MnO	Mn_2O_3	SiO_2	Temperature (°C)
Mn_3O_4(cubic) + Liq.	40	60		1567
Mn_3O_4(cubic) + Mn_3O_4(tetr.)**				1160
Mn_3O_4(tetr.) + Mn_2O_3**				877
Mn_3O_4(cubic) + Teph. + Liq.	54	13	33	1230
Teph. + $MnO \cdot SiO_2$(ss) + Liq.	54	12	34	1206
Mn_3O_4(cubic) + Teph. + $MnO \cdot SiO_2$(ss)				1204
Mn_3O_4(cubic) + Mn_2O_3(ss) + $MnO \cdot SiO_2$(ss)				1168
$MnO \cdot SiO_2$(ss) + Trid. + Liq.	53	5	42	1272
Mn_2O_3(ss) + $MnO \cdot SiO_2$(ss) + Trid.				1048
Trid. + Crist. + Liq.	49	2	49	1470
Crist. + Liq.$_1$ + Liq.$_2$	44 1	1	55 99	1700
Trid. + Crist.**				1470
Crist. + Liq.**			100	1723

* The phase assemblages listed in reality represent univariant situations in the ternary system Mn—Si—O. However, the existing degree of freedom has been "used up" in choosing the O_2 partial pressure of the gas phase, and hence the situations may be considered "invariant".

** "Invariant" situations marked with double asterisk are based on data available in the literature, as follows:

Mn_3O_4(cubic) + Mn_3O_4(tetr.)	Van Hook and Keith, 1958
Mn_3O_4 + Mn_2O_3	Hahn and Muan, in press.
Trid. + Crist.	Sosman, 1955
Crist. + Liq.	Sosman, 1955

Powder X-ray Diffraction Data for Manganese Oxide Containing Crystalline Phases
(Fe Kα Radiation)

Mn_3O_4		Mn_2O_3(ss)		$2MnO \cdot SiO_2$		$MnO \cdot SiO_2$(ss)	
d	I/I_0	d	I/I_0	d	I/I_0	d	I/I_0
4.94	0.3	3.47	0.1	5.34	0.1	3.54	0.3
3.09	0.4	3.33	0.1	4.03	0.3	3.33	0.4
2.88	0.1	2.96	0.1	3.87	0.1	3.13	0.6
2.77	0.9	2.72	1.0	3.63	0.5	3.06	1.0
2.49	1.0	2.36	0.2	3.14	0.3	2.95	0.9
2.37	0.3	2.15	0.2	2.86	0.8	2.75	0.8
2.04	0.3	1.664	0.4	2.70	0.2	2.60	0.5
1.800	0.2			2.61	0.7	2.50	0.2
1.702	0.1			2.56	1.0	2.44	0.1
1.587	0.3			2.45	0.3	2.37	0.2
1.556	0.5			1.893	0.1	2.23	0.2
1.442	0.2			1.824	0.9	2.19	0.2
				1.735	0.2	2.12	0.1
				1.697	0.2	2.08	0.2
				1.570	0.4	1.892	0.1
				1.543	0.3	1.831	0.1
						1.730	0.1

References

Aminoff, G., 1931, Lattice dimensions and space group of braunite: Kungl. Sven. Vetenskapsakad. Hand., v. 9, p. 14-22.

Atlas, Leon, 1952, Polymorphism of $MgSiO_3$ and solid-state equilibria in the system $MgSiO_3$—$CaMgSi_2O_6$: Jour. Geol., v. 60, p. 125-147.

Byström, Anders and Mason, Brian, 1943, The crystal structure of braunite, $3Mn_2O_3 \cdot MnSiO_3$: Arkiv Kemi, Mineral., Geol., v. 16 B, p. 1-8.

Corruccini, R. J., 1949, Differences between the international temperature scales of 1948 and 1927: Jour. Research Natl. Bur. Standards, v. 43, p. 133-146.

Coughlin, J. P., 1954, Contributions to the data on theoretical metallurgy. XII—Heats and free energies of formation of inorganic oxides: U. S. Bur. Mines, Bull. 542.

Dana, J. D., and Dana, E. S., 1944, The system of mineralogy; rewritten by Palache, Charles; Berman, Harry and Frondel, Clifford: New York, John Wiley and Sons, Inc., 7th ed., v. 1., 834 p.

Doerinckel, F., 1911, Untersuchungen über das System Manganoxydul—Kieselsäure: Metallurgie, v. 8, p. 201-211.

Dubois, Pierre, 1934, Hydrate et variétés allotropiques du sesquioxyde de manganèse: Comptes Rendus, v. 199, p. 1416-1418.

Eitel, W., 1957, Structural anomalies in tridymite and cristobalite: Am. Ceram. Soc. Bull., v. 36, p. 142-148.

Fenner, C., 1913, The stability relations of the silica minerals: Am. Jour. Sci., v. 36, p. 331-384.

Flink, Gustav, 1926, Långban and its minerals: Am. Mineralogist, v. 11, p. 195-199.

Flörke, O. W., 1955, Strukturanomalien bei Tridymit und Kristobalit: Ber. deutsch. Keram. Ges., v. 32, p. 369-381.

Fyfe, W. S., 1949, State of manganese in manganese oxides: Nature, v. 164, p. 790.

Glaser, O., 1926, Thermische und mikroskopische Untersuchungen an den für die Kupolofenschlacke bedeutsamen Systemen: MnO—Al_2O_3—SiO_2, MnS—$MnSiO_3$ und CaS—$CaSiO_3$: Cent. für Mineral., Geol. und Palä., Abt. A: Min. und Petrog., p. 81-96.

Glasser, F. P., 1958, The system MnO—SiO_2: Am. Jour. Sci., v. 256, p. 398-412.

Goldschmidt, V. M., 1954, Geochemistry: London, Oxford Univ. Press, 730 p.

Hahn, W. C., and Muan, Arnulf, in press, Studies in the system Mn—O: Am. Jour. Sci.

Herty, C., 1930, Fundamental and applied research on the physical chemistry of steelmaking: Metals and Alloys, v. 1, p. 883-889.

Hill, V. G., and Roy, Rustum, in press, Silica structure studies, VI: On tridymites: Brit. Ceram. Soc. Trans., v. 57, p. 496-510.

Krishnan, K. S., and Banerjee, S., 1939, Magnetic studies on braunite, $3Mn_2O_3 \cdot MnSiO_3$: Zeitschr. Krist., v. 101, p. 507-511.

Magnusson, Nils H., 1924, The Långban minerals from a geological point of view: Geol. Fören. Stockholm Förhandl., p. 284-300.

Muan, Arnulf, 1955, Phase equilibria in the system FeO—Fe_2O_3—SiO_2: AIME Trans., v. 203, p. 965-976; Jour. Metals, Sept., 1955.

————, 1957, Phase equilibria at liquidus temperatures in the system iron oxide—Al_2O_3—SiO_2 in air atmosphere: Am. Ceram. Soc. Jour., v. 40, p. 121-133.

————, 1958, Phase equilibria at high temperatures in oxide systems involving changes in oxidation states: Am. Jour. Sci., v. 256, p. 171-207.

Palache, Charles, 1929, A comparison of the ore deposits of Långban, Sweden, with those of Franklin, New Jersey: Am. Mineralogist, v. 14, p. 43-47.

Pauling, L., and Shappell, M. D., 1930, The crystal structure of bixbyite and the C-modification of the sesquioxides: Zeitschr. Krist., v. 75, p. 128-142.

Roberts, H. S., and Morey, G. W., 1930, Micro-furnace for temperatures above 1000°C: Rev. Sci. Instr., v. 1, p. 576-579.

Sosman, R. B., 1952, Temperature scales and silicate research: Am. Jour. Sci., Bowen Volume, p. 517-528.

Sosman, R. B., 1955, New and old phases of silica: Brit. Ceram. Soc. Trans., v. 54, p. 655-670.

Van Hook, H. J., and Keith, M. L., 1958, The system Fe_3O_4—Mn_3O_4: Am. Mineralogist, v. 43, p. 69-83.

Weyl, W. A., 1956, Acid-base relationship in glass systems. A new acid-base concept applicable to aqueous systems, fused salts, glasses, and solids: The Glass Industry, v. 37, p. 264-269, 286, 288, 325-331, 336, 344, 346, 350.

White, J., Howat, D., and Hay, R., 1934, The binary system MnO—SiO_2: Roy. Tech. Coll. Jour. (Glasgow), v. 3, p. 231-240.

Zachariasen, W., 1928, Über die Kristallstruktur von Bixbyit, sowie vom künstlichen Mn_2O_3: Zeitschr. Krist., v. 67, p. 455-464.